ISSN: 2664-9640

Automatic Detection of Lung Nodules in Computed Tomography (CT) Images: A Systematic Review

Yongbin Li[a], Xinyue Yang[b], Xinqian Chen[c], Enlin Fu[d], Guanghong Ren[e], Yu Mu[f, *]

Faculty of Medical Information Engineering, Zunyi Medical University, Zunyi, Guizhou, China

[a]bynn456@126.com, [b]2570431405@qq.com, [c]3336182038@qq.com, [d]2095764197@qq.com, [e]351454190@qq.com, [f, *]759493522@qq.com

Abstract

Lung cancer is the leading cause of cancer-related mortality worldwide, and early detection of lung nodules is crucial for improving patient survival rates. Computed tomography (CT) is a widely used screening tool for lung cancer, effectively capturing the morphological characteristics of lung nodules. However, the diversity and complexity of lung nodules present challenges for clinical detection and diagnosis. With advancements in deep learning and the availability of large annotated datasets, computer-aided detection (CADe) tools have shown high robustness, sensitivity, and low false-positive rates in lung nodule detection, gradually establishing themselves as mainstream methods in cancer screening. This review summarizes recent research advancements, current trends, and future challenges in automatic lung nodule detection within CT scans, covering studies published up to February 2024. The paper focuses on the techniques involved in various stages of automated lung nodule detection, including commonly used lung parenchyma segmentation methods, lung nodule detection, and false-positive reduction techniques. Finally, the article discusses the challenges faced by current methods and outlines potential future research directions. This review aims to provide researchers with the latest insights into the field of automatic lung nodule detection, advancing the development of early lung cancer diagnosis and treatment.

Keywords

Lung Cancer; Lung Nodule; Automatic Detection; False Positive Reduction; Early Diagnosis; Lung Segmentation.

1. Background

Lung cancer is the most common and deadliest form of cancer globally, claiming approximately 1.3 million lives annually [1]. According to the American Cancer Society's 2023 statistics, an estimated 238,340 individuals in the United States were diagnosed with lung cancer, with 127,070 succumbing to the disease [2]. For cancer patients, the likelihood of survival is significantly influenced by the timing of diagnosis. As lung cancer typically lacks noticeable symptoms in its early stages, around 70% of cases are diagnosed at advanced stages, with a five-year average survival rate of only 16%. However, early detection and timely treatment can increase this five-year survival rate to 70% [3]. Therefore, early detection and treatment are crucial for significantly improving survival rates among lung cancer patients [4].

With advancements in medical technology, computed tomography (CT) has become an effective tool for detecting lung nodules, offering a clear view of lung lesion characteristics and playing a crucial role in the early screening and diagnosis of lung cancer. Lung nodules, often indicative of early-stage lung cancer, are typically defined as circular or irregularly shaped lesions measuring 3mm or larger in diameter. Based on density, lung nodules can be classified into solid and subsolid types [5], with significant variations in size and shape. Due to the variable

ISSN: 2664-9640

morphology of nodules and frequent attachment to blood vessels or airway walls, misdiagnoses can easily occur [6]. Additionally, each patient's CT scan can produce hundreds to thousands of images. According to Doi et al. [7], relying solely on visual screening by radiologists can result in a missed diagnosis rate as high as 30%. To alleviate radiologists' workload and reduce both missed and false diagnoses, researchers have introduced computer-aided detection (CADe) technology to assist radiologists in identifying lung nodules [8].

This study primarily focuses on the nodule detection process within CT imaging. Early lung nodule detection methods relied heavily on manually crafted feature engineering, using characteristics such as shape and texture for nodule recognition [9][10]. While these approaches achieved some success under specific conditions, they faced significant limitations when dealing with complex nodule morphologies and diverse imaging environments. The rapid development of deep learning, particularly convolutional neural networks (CNNs), has brought about a transformative shift in lung nodule detection. Deep learning models can automatically extract relevant features from data and construct end-to-end detection systems, substantially improving detection accuracy and robustness [11][12]. The introduction of these techniques has not only overcome the bottlenecks of manual feature engineering but also steered lung nodule detection from traditional feature-driven approaches toward automated, data-driven models.

This paper systematically reviews the development of lung nodule detection, tracing the evolution from traditional feature engineering methods to the application of modern deep learning techniques. It provides a comprehensive overview of advancements in detection technology, summarizing recent research published as of February 2024 in databases such as IEEE Xplore, Science Direct, PubMed, and Web of Science. The review also delves into current challenges faced by these methods, including data scarcity and model generalization limitations, and explores potential future research directions. The aim is to provide a valuable reference for advancing automated lung nodule detection technologies.

The structure of this review is as follows: Section 2 presents the general CADe framework for lung nodule detection, covering key steps such as image preprocessing, lung parenchyma segmentation, nodule detection, and false positive reduction. Section 3 summarizes commonly used public datasets and their characteristics. Section 4 reviews the evaluation metrics for lung nodule detection, outlining the commonly used performance evaluation standards. Section 5 discusses feature-based methods, including traditional feature engineering and machine learning approaches for lung nodule detection. Section 6 focuses on deep learning-based methods, highlighting recent advancements such as multi-scale feature fusion and attention mechanisms. Section 7 summarizes the challenges faced by current detection methods and suggests future research directions. Finally, Section 8 provides a conclusion for the review.

2. General Framework for Lung Nodule Detection

In the 1980s, researchers began developing computer-aided detection (CAD) systems for identifying lung nodules in CT images [7]. CAD systems can be categorized based on their primary function into detection-aiding (CADe) and diagnosis-aiding (CADx) systems. CADe systems are primarily used for early lung cancer screening and have become a central focus in automated detection research.

This paper focuses on CADe systems for lung nodule detection, outlining the overall implementation process shown in Figure 1, which includes data acquisition, preprocessing, lung segmentation, nodule detection, and false positive reduction. Lung imaging data, typically derived from CT scans, serves as the input for the entire CADe process. Preprocessing is intended to improve image quality through operations like noise filtering [13], histogram correction, and contrast enhancement [14]. Lung segmentation isolates the lung parenchyma

ISSN: 2664-9640

from other anatomical structures, such as bones, mediastinum, and heart tissue [9][15][16][17]. The central component of a CADe system, nodule detection, identifies suspicious nodules within lung images, ensuring high sensitivity, which can result in a substantial number of false positives [9][18][19][20][11]. Finally, false positive reduction is achieved by feature extraction and classifier training [21][22][15][23], eliminating non-nodules to enhance detection accuracy. Together, lung segmentation, candidate nodule detection, and false positive reduction form the core functions of a CADe system.

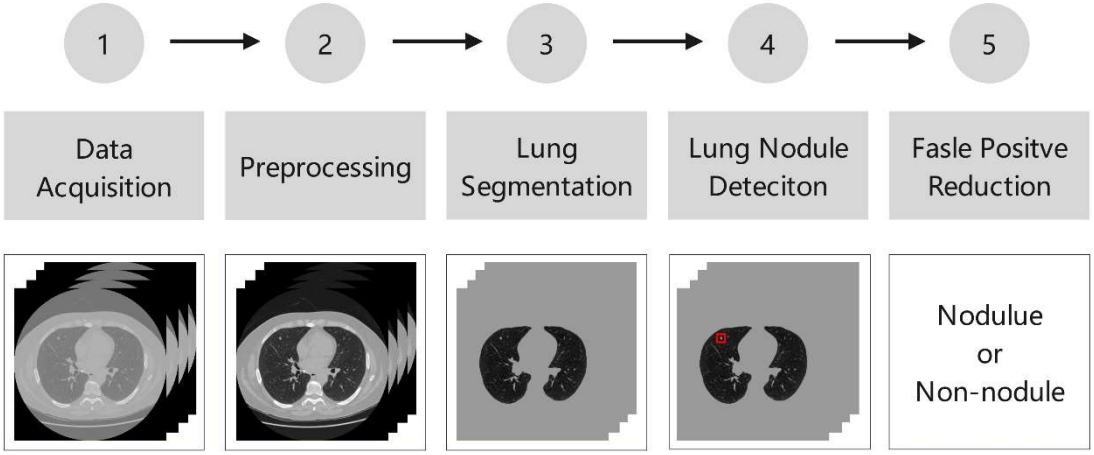

Figure 1. Lung nodule detection process.

3. Dataset

Lung imaging datasets play a critical role in evaluating the performance of lung nodule detection and classification algorithms. In CADe research, some researchers obtain lung CT image data through collaboration with hospitals, which provides invaluable support for research but poses accessibility challenges for others. Additionally, the CT datasets used across studies vary significantly in terms of quality, nodule count, malignancy, size, location, and morphology, making reproducibility and cross-study comparisons challenging. To address these issues, several international organizations have established public databases for standardized evaluation. Commonly used CT databases include: (1) LIDC-IDRI, (2) LUNA16, (3) TianChi, and (4) ANODE09. Below, we provide a detailed overview of each dataset's composition and characteristics.

LIDC-IDRI: The Lung Image Database Consortium and Image Database Resource Initiative (LIDC-IDRI) dataset [24], released by the U.S. National Cancer Institute (NCI) and the National Institutes of Health (NIH) in 2011, is the world's largest publicly available lung nodule dataset, containing 1,018 CT scans with annotated lesions in DICOM format. Diagnostic annotations are provided in XML format. Each CT scan is annotated in two stages by four experienced thoracic radiologists, marking a total of 7,371 nodules, with 2,669 nodules larger than 3 mm in size.

LUNA16: LUng Nodule Analysis 2016 challenge (LUNA16) [25] is a benchmark dataset developed by Setio et al. from LIDC-IDRI data for objective evaluation of automatic lung nodule detection. To improve consistency, LUNA16 excludes CT scans with slice thicknesses exceeding 2.5 mm and retains only nodules annotated by three or four experts. This dataset consists of 888 CT scans with 1,186 annotated nodules. In the false positive reduction challenge, 754,975 candidate nodules are detected using five different methods [26][27][28][29][30], of which 1,557 are true nodules.

TianChi: The TianChi lung nodule dataset [31] was developed as part of the TianChi Medical AI competition, hosted by Alibaba Cloud, Intel, and LinkDoc, and is used to assess the performance of automatic CT lung nodule detection algorithms. The preliminary dataset includes low-dose

ISSN: 2664-9640

CT images from 1,000 high-risk patients, with nodules ranging from 5-10 mm and 10-30 mm in diameter, each accounting for roughly 50% of the nodules. Each nodule was annotated and confirmed by radiologists.

ANODE09: Initiated by the NELSON study group and the University Medical Center Utrecht in the Netherlands, ANODE09 [32] is the largest European CT lung cancer screening database. It contains 55 low-dose CT scan sequences, of which 5 annotated sequences are used for training and 50 unannotated sequences for testing. The annotated scans include 39 nodules and 31 non-nodules, with a slice thickness of 1 mm and pixel spacing between 0.59-0.83 mm, averaging 0.7 mm.

4. Evaluation Metrics

In lung nodule detection tasks, the fundamental evaluation metrics are sensitivity and specificity. Sensitivity measures the model's ability to correctly identify nodules, while specificity indicates the model's accuracy in excluding non-nodules. The formulas for these metrics are as follows:

$$Sensitivity = TP/(TP + FN) \tag{1}$$

$$Specificity = TN/(TN + FP) \tag{2}$$

where TP (true positive) is the count of correctly identified nodules, FN (false negative) represents missed true nodules, TN (true negative) is the number of correctly identified non-nodules, and FP (false positive) is the count of non-nodules incorrectly identified as nodules.

Additionally, the free-response receiver operating characteristic (FROC) curve [33] is a common composite evaluation standard in lung nodule detection. It illustrates the relationship between sensitivity at various thresholds and the average number of false positives per scan (FPs/scan). A curve approaching the top-left corner indicates a model that effectively balances high sensitivity with a low false-positive rate.

For the LUNA16 challenge, the primary evaluation metric, competition performance metric (CPM) [34], was introduced to allow comparative assessment across models. CPM averages sensitivity across predefined FPs/scan thresholds (0.125, 0.25, 0.5, 1, 2, 4, and 8), providing a comprehensive reflection of model performance under various conditions. The CPM is calculated as follows:

$$CPM = \frac{1}{7}\sum_{i=\{0.125,0.25,0.5,1,2,4,8\}} Sensitivity_{fpr=i} \tag{3}$$

where fpr denotes FPs/scan, and $Sensitivity_{fpr=i}$ is the sensitivity at a specific FPs/scan threshold i.

5. Feature-Based Lung Nodule Detection

In lung nodule detection, traditional feature-based methods generally rely on manually designed features, such as shape, texture, and density, combined with machine learning algorithms to perform detection. These methods typically include four main steps: image preprocessing to enhance quality, segmentation of the lung region to exclude irrelevant tissues, nodule detection to identify suspicious regions, and false positive reduction to improve detection accuracy.

ISSN: 2664-9640

However, these approaches have limitations in capturing the complexity and variability of nodules, particularly for small or irregularly shaped nodules, often resulting in missed detections or false positives. Additionally, these methods depend heavily on expert-driven feature design, which hinders adaptability to datasets with varying imaging conditions and reduces generalizability. Although traditional methods have shown some effectiveness under specific conditions, their performance remains inconsistent and sensitive to variations in data diversity.

5.1. Preprocessing

In traditional lung nodule detection methods, preprocessing is an essential initial step aimed at enhancing CT image quality, providing clearer inputs for subsequent algorithms. Common preprocessing techniques apply traditional image processing methods to reduce noise and improve image contrast, highlighting details of lung structures [9][13][14][27][35][36][37]. For instance, Arimura et al. [13] employed noise correction and smoothing filters to improve image quality; Messay et al. [9] and Liu et al. [36] used enhancement filters to increase CT image contrast. Ashwin et al. [14] applied histogram equalization to further enhance image contrast, while Setio et al. [27] introduced Gaussian filtering for CT resampling to achieve isotropic resolution. Additionally, Shao et al. [37] used Wiener filtering to implement automatic image enhancement.

5.2. Lung Segmentation

CT imaging captures the entire thoracic region, encompassing not only lung tissue but also surrounding structures such as blood vessels, bronchi, and extrathoracic tissues. Lung segmentation focuses on isolating the lung region within CT scans, minimizing interference from surrounding tissues and reducing computational load. Traditional image processing techniques, including thresholding [9][21][38][39][40][41], region-based [15][42][43][44][45], and shape-based methods [16][46][47][48], are commonly applied for lung segmentation.

Thresholding methods exploit the grayscale differences between lung parenchyma and other anatomical structures due to varying densities. For instance, Messay et al. [9] employed a fixed CT value for threshold segmentation of the lung region, while other studies utilized optimal thresholds [21][38], multi-threshold techniques [39], edge detection integration [40], and connected component labelling [41]. Although thresholding is efficient, it struggles with extensive bright pathological regions. Region-based segmentation leverages the similarity within regions, using techniques such as region growing [15], watershed [42], graph cuts [43], random walks [44], and fuzzy connectivity (FC) [45]. For example, Naqi et al. [15] combined region growing and thresholding to exclude the background and applied differential evolution for boundary extraction. Dai et al. [43] used a Gaussian mixture model-based graph cut for segmenting juxtapleural nodules, while Mansoor et al. [45] implemented fuzzy connectivity for pathological region segmentation. However, these methods are sensitive to seed points and can be time-consuming. Shape-based segmentation methods incorporate prior anatomical knowledge, with models such as atlas-based approaches [16], active contour models [46][47], and level sets [48]. Oliveira et al. [16] utilized a multi-atlas strategy for CT lung segmentation, while Filho et al. [46] applied a 3D active contour model. These methods, however, rely heavily on registration parameters and initial model placement.

To adapt to complex clinical scenarios, some researchers combine multiple methods to enhance segmentation robustness [35][49][50][51][52]. For example, Ye et al. [35] generated an initial lung template with 3D adaptive fuzzy thresholding, then refined the boundary using chain codes. Taşcı et al. [49] applied Otsu thresholding with morphological operations for lung extraction, and Liu et al. [50] combined region growing and thresholding for lung segmentation.

ISSN: 2664-9640

Shi et al. [51] used a hybrid of thresholding, region growing, and random walks, while Chen et al. [52] integrated graph cuts and active modeling for efficient lung segmentation.

5.3. Lung Nodule Detection

Lung nodule detection aims to identify potential nodule regions within segmented lung images for further screening and diagnosis. Traditional nodule detection methods based on hand-crafted features mainly include thresholding and morphological operations [9][18][19][20][53], edge detection methods [54], fuzzy set-based detection methods [10], clustering-based detection methods [55], and energy optimization-based detection methods [56].

Messay et al. [9] paired multiple thresholds with specific morphological operations to eliminate irrelevant tissue around nodules. Paing et al. [18] proposed a nodule detection method combining OTSU algorithm with morphological operations. EI-Regaily et al. [19] developed a method that integrates region-growing, thresholding, and morphological operations to detect and segment nodules, achieving a detection rate of 77.77% with 4.1 FPs/scan. Additionally, Gupta et al. [20] used a flood-fill algorithm and morphological operations to obtain lung masks, followed by a multi-threshold processing algorithm combined with feature extraction techniques to detect nodules. Similarly, John et al. [53] applied multi-threshold and feature extraction methods for nodule detection.

For edge detection methods, Rezaie et al. [54] first applied a thresholding method to select suspicious nodule regions of interest, then used edge detection algorithms to precisely locate them. Lu et al. [10] developed an integrated nodule detection algorithm that combines morphological operations, Hessian matrix, fuzzy sets, and regression trees. Javaid et al. [55] used K-means clustering for initial nodule detection and segmentation, followed by spherical morphological opening operations to further refine the results. Wang et al. [56] applied gray-level enhancement and spherical enhancement filters to extract spherical contours, and finally used a shape-constrained Chan-Vese model for false-positive reduction, improving detection accuracy.

5.4. False Positive Reduction

To further reduce the interference of false positive nodules, various classifiers are often introduced after feature extraction to distinguish between nodules and non-nodules. Common classifiers in the false positive reduction stage include rule-based filters [35], Linear Discriminant Analysis (LDA) [9][26], Support Vector Machine (SVM) [21][22][35][38][57][58], Random Forest (RF) [59], K-Nearest Neighbors (KNN) [28], and Conditional Random Field (CRF) [50].

For example, Choi et al. [21] achieved a true positive rate of 97.5% with an SVM classifier using surface features based on the Hessian matrix when FPs/scan was 6.76. Filho et al. [22] utilized 3D shape and ratio features to identify suspicious nodules and used an SVM to classify them as true or false nodules. Ye et al. [35] detected nodule regions using shape indices and point features, combining rule-based filters with an SVM classifier to achieve a detection rate of 90.2% at FPs/scan of 8.2. Liu et al. [59] used a fuzzy C-means algorithm for initial detection, followed by RF classification using 22 texture and shape features, achieving a recall rate of 94.8% at FPs/scan of 4.5. Murphy et al. [28] extracted candidate structures based on shape indices and curvature features and used two consecutive KNN classifiers to reduce false positives, achieving a sensitivity of 80% at FPs/scan of 4.2. Liu et al. [50] also employed a hidden CRF to classify 3D candidate nodules, enhancing detection sensitivity.

In recent years, researchers have improved true positive rates and reduced false positive counts by combining multiple features and integrating different classifiers [10][15][38][60][61]. For instance, Naqi et al. [15] mixed geometric and texture features into a

ISSN: 2664-9640

feature vector and used an ensemble of SVM classifiers with linear, polynomial, and Gaussian radial basis function kernels, achieving 99.0% accuracy, 98.6% true positive rate, and 98.2% true negative rate at FPs/scan of 3.4 on a dataset of 250 cases containing 567 nodules. Shaukat et al. [38] combined intensity, shape (2D and 3D), and texture features with SVM to classify lung nodules, achieving detection and classification sensitivities of 94.20% and 98.15%, respectively, with only 2.19 false positives per scan. Despite the success of traditional detection algorithms, challenges remain in terms of generalizability and efficiency, with limitations in handling diverse datasets and slow processing speeds.

6. Deep Learning-based Lung Nodule Detection

In recent years, deep learning has advanced rapidly in the field of image processing and has become a mainstream method due to its strong self-learning and expressive capabilities. In lung nodule detection specifically, convolutional neural network (CNN)-based deep learning models have become a prominent research focus for their ability to effectively learn from large-scale image data [11][62][63]. CNN-based lung nodule detection methods can autonomously learn relevant nodule features, effectively replacing manually crafted shape and texture features, thus enabling end-to-end training of nodule detection models. Compared to traditional methods, CNN-based models offer significantly improved generalization ability [12].

6.1. Overview of CNN-based Methods

A typical example of 2D CNN detection methods is demonstrated by Golan et al. [11], who achieved a sensitivity of 78.9% at 20 FPs/scan using a 2D CNN without any segmentation or additional false-positive reduction measures. However, since lung CT images consist of hundreds of cross-sectional slices forming a 3D structure, using 2D CNNs for lung nodule detection fails to capture the spatial characteristics of nodules. To better preserve the three-dimensional attributes of CT imagery, lung nodule detection research has gradually shifted from 2D CNNs to 3D CNNs.

With Anirudh et al. [64] introducing 3D convolutional kernels to nodule detection, the application of 3D CNNs in this field has gained significant traction [12][23][65][66][67][68]. Representative 3D CNN-based methods include Jenuwine et al. [65], who developed a 3D CNN-based detection system that efficiently identifies nodules in CT images without requiring additional false positive filtering. Perez et al. [66] achieved a sensitivity of 99.6% and an AUC of 0.913 using a 3D CNN on the LIDC-IDRI dataset. Dou et al. [23] applied a 3D CNN with an online sample filtering approach for nodule detection, followed by a residual network for false positive reduction, achieving a CPM score of 83.9%. Huang et al. [67] utilized prior knowledge of nodule anatomy to generate suspicious nodules through a local geometry-based filter, then classified nodules using a 3D CNN. Mei et al. [12] designed a slice-aware network (SA-Net) to implement two-stage lung nodule detection, where a feature extractor and RPN generate candidate nodules, followed by a multi-scale feature-based false positive reduction module to re-identify and adjust candidate positions. Similarly, Cao et al. [68] developed a two-stage detection architecture, first applying a ResDense-based U-Net for nodule detection, then reducing false positives through an ensemble 3D CNN architecture, yielding competitive performance on the LUNA16 dataset. Additionally, models such as ResNet [69], 3D ResNet [70], and DenseNet [71] are widely used for feature extraction and nodule detection. For instance, Han et al. [72] used a 3D CNN model to detect candidate lung nodules, classifying them as intrapulmonary or pleural nodules with a detection accuracy of 0.879 at 1 FP/scan in the LNPE1000 dataset. Khosrava et al. [73] introduced a densely connected 3D CNN that achieved a CPM score of 0.897 without further post-processing.

Table 1 showcases recent advancements in the application of deep learning techniques for lung nodule detection. With enhanced computational resources and the widespread adoption of

ISSN: 2664-9640

deep learning, an increasing number of researchers have employed CNN models and their variants, such as 2D and 3D CNNs, ResNet, and DenseNet, for lung nodule detection in CT imaging. These models automatically learn spatial features of nodules, overcoming the limitations of manually designed features and significantly improving detection accuracy and generalization. Overall, 2D CNN methods achieve rapid detection with low computational cost, making them suitable for detecting simpler or more clearly defined nodules. In contrast, 3D CNNs capture the three-dimensional information of CT images, preserving spatial characteristics of nodules and demonstrating higher accuracy in detecting nodules with complex structures.

Table 1. Overview of Recent Deep Learning-Based Approaches for Lung Nodule Detection.

Reference	Year	Method	Datasets	Results
Golan et al. [11]	2016	2D CNN	LIDC-IDRI	Sensitivity 78.9% at 20 FPs/scan
Dou et al. [23]	2017	3D CNN	LUNA16	CPM: 0.839
Huang et al. [67]	2017	3D CNN	LIDC-IDRI	Sensitivity 90.0% at 5 FPs/scan
Ding et al. [81]	2017	Faster RCNN	LUNA16	CPM: 0.893
Khosravan et al. [73]	2018	3D CNN with dense connection	Luna16	CPM: 0.897
Ramachandran et al. [62]	2018	YOLO	LIDC-IDRI	Sensitivity 89% at 6 FPs/scan
Zhu et al. [74]	2018	3D CNN	LUNA16	CPM: 0.842
Xie et al. [80]	2019	Faster RCNN	LUNA16	Sensitivity: 86.42%
Tang et al. [82]	2019	NoduleNet	LIDC-IDRI	CPM: 0.8727
Perez et al. [66]	2020	3D CNN	LIDC-IDRI	Sensitivity: 99.6%, Accuracy:91.3%
Li et al. [88]	2020	3D CNN with SE attention	LUNA16	CPM: 0.862
Cao et al. [68]	2020	ResDense-based U-Net	LUNA16	CPM: 0.911
Tang et al. [84]	2020	Multi-scale 3D U-Net and transfer learning	LUNA16 Tianchi	Sensitivity: 90.4%, Accuracy:96.8% Specificity: 94.6%, AUC: 94.1%
Zheng et al. [85]	2020	Multi-scale 3D CNN	LUNA16	CPM: 0.906
Peng et al. [87]	2021	Multi-scale 3D CNN	LUNA16	CPM: 0.923
Mei et al. [12]	2021	slice-aware CNN	LUNA16 PN9	CPM:0.874 in LUNA16 CPM:0.645 in PN9
Luo et al. [89]	2021	anchor-free 3D CNN	LUNA16	CPM: 0.892
Huang et al. [90]	2022	3D OSAF-YOLOv3	LUNA	CPM: 0.905
Bu et al. [77]	2022	YOLO V3	RIDER	Accuracy: 95.17%
Han et al. [72]	2022	3D CNN	LNPE1000	Accuracy: 87.9%
Zhao et al. [86]	2022	Multi-scale faster RCNN	LUNA16	CPM: 0.829
Zhao et al. [91]	2023	3D CNN with Channel and spatial attention	LUNA	CPM: 0.848
Cao et al. [92]	2023	Multi-scale 3D CNN with attention	LUNA16	mAP:83.08%
Mkindu et al. [94]	2023	3D CNN with channel attention	LUNA16	CPM: 0.911 Sensitivity: 98.65%
UrRehman et al. [93]	2024	2D CNN with channel and spatial attentions	LUNA16	Sensitivity: 94.69%, Accuracy: 94.40% Specificity: 93.17%, AUC of 98.00%

6.2. Single-Stage and Two-Stage Detection Models

CNN-based lung nodule detection models can generally be divided into single-stage and two-stage models. Single-stage models treat nodule detection as a regression task, directly estimating the location and classification of nodules from images, offering high detection speed and sensitivity. For instance, Zhu et al. [74] designed a single-stage detection model with a 3D

ISSN: 2664-9640

dual-path network (DPN) and encoder-decoder architecture, achieving a CPM score of 84.2%. You Only Look Once (YOLO) [75] and Single Shot MultiBox Detector (SSD) [76] are popular single-stage object detection models and have been widely applied in medical image detection. Ramachandran et al. [62] developed a YOLO-based real-time deep network for lung nodule detection, achieving a recall rate of 89% at 6 FPs/scan. Bu et al. [77] further enhanced YOLOv3 [78] by augmenting the dataset with random geometric transformations and Poisson blending, training on 419 RIDER dataset slices, which reduced detection time by 2-3 times with an accuracy of 95.17%.

Two-stage detection models, exemplified by Faster R-CNN [79], introduce an innovative Region Proposal Network (RPN) to generate candidate regions, integrating feature extraction, classification, and regression tasks. Improvements to Faster R-CNN include methods like Xie et al. [80], who implemented a dual RPN with deconvolution layers, achieving a recall rate of 86.4% at 2 FPs/scan. Ding et al. [81] developed a Faster R-CNN with deconvolution architecture, detecting suspicious nodules at each layer, followed by 3D CNN-based false-positive reduction, reaching a CPM score of 0.893. Tang et al. [82] introduced the NoduleNet framework, which integrates U-Net backbone features with two branches designed for false-positive reduction and candidate segmentation, achieving end-to-end multi-task learning.

6.3. Multi-Scale Fusion Methods

In lung CT imaging, nodules typically occupy a small volume with significant variability in size and shape, presenting challenges for deep learning-based feature extraction. Consequently, some researchers have turned to multi-scale feature extraction for lung nodule detection [84][85][86][87]. Tang et al. [84] proposed a 3D U-Net-based multi-scale transfer learning method for automatic lung nodule detection in chest CTs. This approach demonstrated robust performance on the LUNA16 and TianChi datasets, achieving high accuracy in detecting medium and large nodules and over 70% accuracy for small nodules. Zheng et al. [85] built a multi-scale feature detection network combined with a candidate scoring network to develop an end-to-end CADe system for lung nodules. Furthermore, Zhao et al. [86] integrated multi-scale features with a Faster R-CNN framework to enhance the detection of small nodules and designed a 3D CNN based on multi-scale fusion for false-positive suppression, achieving a sensitivity of 0.905 and a CPM score of 0.829 at 4 FPs/scan on the LUNA16 dataset. Peng et al. [87] introduced a 3D multi-scale CNN named Res2SENet, incorporating squeeze-and-excitation units into Res2Net residual blocks to create a 3D candidate nodule detection network and a false-positive reduction network, achieving an average sensitivity of 0.923 on the LUNA16 dataset.

Multi-scale fusion methods demonstrate significant advantages in lung nodule detection, particularly for nodules with varied sizes and shapes. Traditional single-scale feature extraction methods often fail to capture the details of small or faintly-bordered nodules, while multi-scale feature fusion effectively addresses this limitation by integrating features at multiple resolutions. This enhances the model's accuracy and robustness in nodule identification while improving generalizability across datasets. However, multi-scale fusion methods are computationally intensive and require substantial resources. Balancing performance with model simplification and efficiency remains a key area for future research.

6.4. Attention Mechanism-Based Detection Methods

In recent years, the success of attention mechanisms in deep learning has led researchers to apply these techniques to lung nodule detection as well [87][88][89][90][91][92][93][94]. Li et al. [88] introduced an end-to-end 3D deep CNN with an encoder-decoder structure (DeepSEED) for nodule detection, integrating a squeeze-and-excitation (SE) attention module [95] into the residual blocks, significantly improving detection performance. Luo et al. [89] proposed an anchor-free 3D spherical representation network (3D-SCPM-Net) designed to capture spatial

ISSN: 2664-9640

and 3D contextual information for detection. This network fuses multi-level spatial coordinate maps with feature extractors, combining them with a 3D SE attention module, resulting in a CPM score of 0.892 on the LUNA16 dataset. Further advancements were made by Huang et al. [90], who applied feature fusion and attention mechanisms to a single-stage 3D DCNN, achieving remarkable performance on CT images for lung nodule detection. Zhao et al. [91] proposed a novel 3D CNN architecture incorporating both channel and spatial attention in a multi-scale framework, adding multi-scale feature extraction modules and attention mechanisms to residual blocks in a 3D Fast-R-CNN, which was enhanced with a U-Net-based region proposal network. This approach achieved a CPM score of 0.848 on the LUNA16 dataset. Additionally, Cao et al. [92] employed color enhancement strategies for grayscale images, adding contextual information, and designed an attention-based ResSCBlock module for feature extraction, integrating feature pyramid network (FPN) [83] for feature fusion. This boosted the prediction capability for small nodules, achieving a mAP of 83% on the LUNA16 dataset. UrRehman et al. [93] developed a dual attention mechanism combining channel and spatial attention, effectively highlighting essential features and custom-tailoring the CNN for improved efficiency and accuracy in lung nodule diagnosis.

Overall, the integration of attention mechanisms has enhanced the ability of lung nodule detection models to capture spatial information and extract features, proving particularly effective in handling nodule size and shape variability and in reducing false positives. In the future, combining attention mechanisms with multi-scale feature fusion is expected to further optimize model performance, providing more reliable support for early diagnosis.

6.5. CNN-Based False Positive Reduction

In addition, several studies have focused on reducing false positives in nodule detection by using CNNs to construct candidate classification networks [63][96][97][98][99][100], with representative works shown in Table 2. For example, Fu et al. [63] trained a CNN network by combining lung CT images, enhanced nodule images, and vascular images, integrating manually designed grayscale, shape, and texture features with deep features for candidate nodule classification. Eun et al. [96] proposed an integrated single-view 2D CNN-based false positive reduction framework, achieving a CPM score of 0.922 on the LUNA16 dataset. Setio et al. [97] utilized a multi-view CNN to extract 2D patches from different angles of candidate nodules, achieving sensitivities of 85.4% and 90.1% at 1 and 4 FPs/scan, respectively, on the LIDC-IDRI dataset. Recognizing the 3D nature of CT images, some studies have aimed to better leverage three-dimensional information. For example, Dou et al. [98] adopted multi-scale 3D inputs, training three 3D CNNs independently on different input scales, then linearly weighted the outputs from the networks. Zuo et al. [99] proposed a 3D CNN with multiple embedded branches, each handling feature maps of different depths, with these branches concatenated at the end for candidate nodule classification. Their approach achieved a CPM score of 0.830 on the LUNA16 dataset. Yuan et al. [100] developed a hierarchical structure to extract spatial information from candidate nodules and connected three pathways with varying receptive fields within a 3D CNN model. This effectively captured and fused spatial, size, and contextual information of nodules, yielding a CPM score of 0.881 and a sensitivity of 95.2% at 4 FPs/scan on the LUNA16 dataset.

Some studies have also incorporated multi-scale features and attention mechanisms to reduce false positives in lung nodule detection [101][102][103][104][105][106][107][108]. For instance, Kim et al. [101] used a progressive integration strategy to fuse multi-scale 3D inputs and applied CNNs to suppress false-positive nodules. Mittapalli et al. [102] proposed a multi-scale CNN with compound fusion (MCNN-CF) that uses multi-scale 3D patches as input and performs intermediate feature fusion at different network depths, achieving a CPM score of 0.948 on the LUNA16 dataset. Zhao et al. [103] introduced a novel multi-scale CNN that

ISSN: 2664-9640

integrates spatiotemporal and frequency-domain information to reduce false positives. Vipparla et al. [104] developed an attention-based multi-patch 3D CNN with a hybrid fusion architecture, reaching a CPM score of 0.931 on LUNA16. Gu et al. [105] proposed a cross-attention-guided multi-scale feature fusion method, achieving a CPM of 0.848 on the LUNA16 dataset. Sun et al. [106] introduced an attention-embedded complementary-stream convolutional neural network (AECS-CNN), utilizing progressive multi-scale feature extraction blocks with attention modules to capture contextual information and complementary feature blocks with attention to enhance important features, achieving a sensitivity of 92% at 4 FPs/scan on the LUNA16 dataset.

Table 2. Overview of Deep Learning-Based False Positive Reduction Methods in Lung Nodule Detection.

Reference	Year	Method	Datasets	Results
Fu et al. [63]	2017	2D CNN	LIDC-IDRI	Sensitivity: 90.9% at 4 FPs/scan
Setio et al. [97]	2016	Multi-view 2D CNN	LIDC-IDRI	CPM: 0.838
Dou et al. [98]	2017	Multi-level contextual 3D CNN	LUNA	CPM:0.908
Eun et al. [96]	2018	Single-view 2D CNN	LUNA	CPM:0.922
Xiao et al. [107]	2019	Multi-scale heterogeneous 3D CNN	LUNA	CPM:0.929
Kim et al. [101]	2019	MGI-CNN	LUNA	CPM: 0.942
Cao et al. [109]	2019	Multi-branch ensemble learning 3D CNN	LUNA	CPM:0.878
Zuo et al. [99]	2020	Multi-branch 3D CNN	LUNA	CPM:0.830 Sensitivity: 87.71%, accuracy: 97.83% Specificity: 99.25%, precision: 94.26%
Mittapalli et al. [102]	2021	Multiscale CNN with compound fusions	LUNA	CPM: 0.948
Sun et al. [106]	2021	attention-embedded complementary-stream CNN	LUNA	CPM:0.762
Yuan et al. [100]	2021	multi-path 3D CNN	LUNA	CPM: 0.881
Vipparla et al. [104]	2021	Multi-Patched 3D-CNN with Hybrid Fusion Architecture	LUNA	CPM:0.931
Haiying et al. [110]	2021	Deformable CNN	LUNA	CPM:0.835
Zhao st al. [103]	2022	Multi-scale 2D CNN	LUNA	CPM:0.896 Sensitivity: 95.2%, accuracy: 96.7% Specificity: 98.1%, F1-score: 93.9%
Gu et al. [105]	2022	Cross attention guided multi-scale 3D-CNN	LUNA	CPM: 0.848
Hao et al. [108]	2023	central attention CNN	LUNA	Sensitivity: 92.64%, specificity: 98.71% accuracy: 98.69%, AUC: 95.67%

7. Challenges and Future Directions

This review explored the advancements in deep learning for lung nodule detection and false positive reduction from 2016 to 2024, summarizing the contributions of various models in lung CT image analysis, as illustrated in Tables 1 and 2. While significant progress has been made in lung nodule detection based on CT images, several challenges remain for clinical application. Based on existing studies, this section highlights three core challenges: the variability in nodule shape and size, the scarcity of labeled training data, and the computational costs of real-time detection. Corresponding future research directions are proposed.

ISSN: 2664-9640

Firstly, the diversity in nodule shape and size remains a major difficulty in lung nodule detection. Nodules vary considerably in their appearance, with differences in size, shape, and density, especially for smaller nodules, which can be easily confused with normal structures such as blood vessels and pleuras like multi-scale feature extraction and attention mechanisms address some of these variations, current methods cannot fully account for the diversity in nodule characteristics. Future research could explore adaptive multi-scale fusion strategies that dynamically adjust feature weights to improve the detection accuracy of complex nodules. Integrating context-aware multi-scale network architectures and advanced feature enhancement techniques, such as pyramid attention mechanisms combined with image segmentation, could further capture both local features and global context, enhancing model detection performance.

Secondly, the scarcity of training data poses a critical challenge for deep learning techniques. Training deep learning models typically requires a large volume of annotated medical images, but collecting such extensive labeled datasets is both time-consuming and costly, even for skilled radiologists. To mitigate this limitation, researchers have introduced various approaches, such as transfer learning and computer-generated images. Transfer learning leverages models pre-trained on large datasets to address small sample size issues, while generative adversarial networks (GANs) can produce synthetic images to expand training datasets. For better model generalization, future research could incorporate weakly supervised and multi-task learning strategies to maximize the utility of limited labeled data.

Lastly, the computational demands of real-time detection remain a bottleneck in applying deep learning to lung nodule detection. With the increasing complexity of models, including deep networks, multi-scale feature fusion, and attention mechanisms, the need for computational resources has grown significantly, especially in large-scale CT screening. Researchers have investigated techniques to reduce computational loads, such as lightweight network designs (e.g., MobileNet, ShuffleNet) and efficient model optimization strategies. Moreover, model pruning and quantization can reduce parameter counts and computational costs while maintaining detection accuracy, and mixed-precision computation and hardware acceleration (e.g., GPUs and TPUs) aid in speeding up inference to achieve real-time detection. Future studies could further refine these techniques, aiming to develop efficient real-time detection systems to meet clinical application needs.

In conclusion, despite the notable advancements in lung nodule detection, the challenges of nodule shape and size diversity, limited training data, and computational costs for real-time detection remain unresolved. Future research should focus on innovative solutions to these challenges, advancing the application of automated detection technology in clinical settings.

8. Conclusion

This paper reviewed recent advancements in deep learning methods for lung nodule detection and false positive reduction, focusing on studies published from 2016 to 2024. Our investigation highlighted that CNNs remain the most widely used deep learning technology for nodule detection and classification. Building on CNNs, researchers have employed multi-scale feature extraction and attention mechanisms to enhance detection performance. The literature shows that CADe systems based on deep learning effectively improve both lung nodule detection and false positive reduction, demonstrating considerable potential for clinical application and being gradually integrated into diagnostic practices. However, challenges such as data scarcity and the difficulty of detecting small nodules persist. Despite these limitations, with the rapid evolution of technology and growth in the medical industry, deep learning is expected to meet the rising demand for precision diagnostics in healthcare.

ISSN: 2664-9640

Acknowledgments

This work was supported by the Youth Science and Technology Talent Growth Project of Ordinary Higher Education Institutions in Guizhou Province (Qianjiaohe KY[2022] No. 281); Guizhou Province College Innovation and Entrepreneurship Training Program (S2024106612376); Zunyi Medical University Undergraduate Innovation and Entrepreneurship Training Program (ZYDC202402321); Zunyi Medical University Undergraduate Innovation and Entrepreneurship Training Program (ZYDC202402337).

References

[1] Siegel R L, Miller K D, Jemal A. Cancer statistics, 2018[J]. CA: a cancer journal for clinicians, 2018, 68(1): 7-30.

[2] Siegel RL, Miller KD, Wagle NS, Jemal A. Cancer statistics, 2023. CA Cancer J Clin. 2023 Jan; 73(1):17-48. doi: 10.3322/caac.21763. PMID: 36633525.

[3] Baldwin DR. Prediction of risk of lung cancer in populations and in pulmonary nodules: significant progress to drive changes in paradigms. Lung Cancer 2015; 89:1-3.

[4] Wood D E, Kazerooni E A, Baum S L, et al. Lung cancer screening, version 3.2018, NCCN clinical practice guidelines in oncology[J]. Journal of the National Comprehensive Cancer Network, 2018, 16(4): 412-441.

[5] Zheng S, Cornelissen L J, Cui X, et al. Deep convolutional neural networks for multiplanar lung nodule detection: Improvement in small nodule identification[J]. Medical physics, 2021, 48(2): 733-744.

[6] Gould M K, Donington J, Lynch W R, et al. Evaluation of individuals with pulmonary nodules: When is it lung cancer?: Diagnosis and management of lung cancer: American College of Chest Physicians evidence-based clinical practice guidelines[J]. Chest, 2013, 143(5): e93S-e120S.

[7] Doi K. Computer-aided diagnosis in medical imaging: historical review, current status and future potential[J]. Computerized medical imaging and graphics, 2007, 31(4-5): 198-211.

[8] Firmino M, Morais A H, Mendoça R M, et al. Computer-aided detection system for lung cancer in computed tomography scans: review and future prospects[J]. Biomedical engineering online, 2014, 13: 1-16.

[9] Messay T, Hardie R C, Rogers S K. A new computationally efficient CAD system for pulmonary nodule detection in CT imagery [J]. Medical image analysis, 2010, 14(3): 390-406.

[10] Lu L, Tan Y, Schwartz L H, et al. Hybrid detection of lung nodules on CT scan images[J]. Medical physics, 2015, 42(9): 5042-5054.

[11] Golan R, Jacob C, Denzinger J. Lung nodule detection in CT images using deep convolutional neural networks[C]. 2016 International Joint Conference on Neural Networks (IJCNN). IEEE, 2016.

[12] Mei J., Cheng M.M., Xu G., Wan L.R., Zhang H. SANet: A slice-aware network for pulmonary nodule detection. IEEE Trans. Pattern Anal. Mach. Intell. 2021 doi: 10.1109/TPAMI.2021.3065086.

[13] Arimura H, Magome T, Yamashita Y, et al. Computer-aided diagnosis systems for brain diseases in magnetic resonance images[J]. Algorithms, 2009, 2(3): 925-952.

[14] Ashwin S, Ramesh J, Kumar S A, et al. Efficient and reliable lung nodule detection using a neural network based computer aided diagnosis system[C]//2012 International Conference on Emerging Trends in Electrical Engineering and Energy Management (ICETEEEM). IEEE, 2012: 135-142.

[15] Naqi S M, Sharif M, Yasmin M. Multistage segmentation model and SVM-ensemble for precise lung nodule detection[J]. International journal of computer assisted radiology and surgery, 2018, 13: 1083-1095.

[16] Oliveira B, Queirós S, Morais P, et al. A novel multi-atlas strategy with dense deformation field reconstruction for abdominal and thoracic multi-organ segmentation from computed tomography[J]. Medical Image Analysis, 2018, 45: 108-120.

ISSN: 2664-9640

[17] Dou Q, Yu L, Chen H, et al. 3D deeply supervised network for automated segmentation of volumetric medical images[J]. Medical image analysis, 2017, 41: 40-54.

[18] Paing M P, Choomchuay S. A computer aided diagnosis system for detection of lung nodules from series of CT slices[C]//2017 14th International Conference on Electrical Engineering/Electronics, Computer, Telecommunications and Information Technology (ECTI-CON). IEEE, 2017: 302-305.

[19] El-Regaily S A, Salem M A M, Aziz M H A, et al. Lung nodule segmentation and detection in computed tomography[C]//2017 Eighth International Conference on Intelligent Computing and Information Systems (ICICIS). IEEE, 2017: 72-78.

[20] Gupta A, Martens O, Le Moullec Y, et al. Methods for increased sensitivity and scope in automatic segmentation and detection of lung nodules in CT images[C]//2015 IEEE International Symposium on Signal Processing and Information Technology (ISSPIT). IEEE, 2015: 375-380.

[21] Choi W J, Choi T S. Automated pulmonary nodule detection based on three-dimensional shape-based feature descriptorv [J]. Computer methods and programs in biomedicine, 2014, 113(1): 37-54.

[22] Filho A O C, Silva A C, de Paiva A C, et al. 3D shape analysis to reduce false positives for lung nodule detection systems[J]. Medical & biological engineering & computing, 2017, 55: 1199-1213.

[23] Dou Q., Chen H., Jin Y., et al. Automated Pulmonary Nodule Detection via 3D ConvNets with Online Sample Filtering and Hybrid-Loss Residual Learning BT - Medical Image Computing and Computer-Assisted Intervention – MICCAI 2017. DESCOTEAUX M, MAIER-HEIN L, FRANZ A, et al. Cham: Springer International Publishing, 2017:630-638

[24] Armato III S G, McLennan G, Bidaut L, et al. The lung image database consortium (LIDC) and image database resource initiative (IDRI): a completed reference database of lung nodules on CT scans[J]. Medical physics, 2011, 38(2): 915-931.

[25] Setio A.A.A., Traverso A., De Bel T., Berens M.S., Van Den Bogaard C., Cerello P., Chen H., Dou Q., Fantacci M.E., Geurts B., et al. Validation, comparison, and combination of algorithms for automatic detection of pulmonary nodules in computed tomography images: The LUNA16 challenge. Med. Image Anal. 2017; 42:1–13. doi: 10.1016/j.media.2017. 06.015.

[26] Jacobs C, Van Rikxoort E M, Twellmann T, et al. Automatic detection of subsolid pulmonary nodules in thoracic computed tomography images [J]. Medical image analysis, 2014, 18(2): 374-384.

[27] Setio A A A, Jacobs C, Gelderblom J, et al. Automatic detection of large pulmonary solid nodules in thoracic CT images[J]. Medical physics, 2015, 42(10): 5642-5653.

[28] Murphy K, van Ginneken B, Schilham A M R, et al. A large-scale evaluation of automatic pulmonary nodule detection in chest CT using local image features and k-nearest-neighbour classification[J]. Medical image analysis, 2009, 13(5): 757-770.

[29] Tan, M.; Deklerck, R.; Jansen, B.; Bister, M.; Cornelis, J. A Novel Computer-Aided Lung Nodule Detection System for CT Images. Med. Phys. 2011, 38, 5630–5645.

[30] Traverso, A.; Torres, E.L.; Fantacci, M.E.; Cerello, P. Computer-Aided Detection Systems to Improve Lung Cancer Early Diagnosis: State-of-the-art and Challenges. In Proceedings of the 7th Young Researcher Meeting, Torino, Italy, 24–26 October 2016.

[31] Tianchi medical AI competition: Intelligent diagnosis of pulmonary nodules [DB/OL].https:// TIANCHI.aliyun. com/competition /introduction. htm? spm = 5176. 10006 6.0.0.334 cd780jWtEiJ&raceId = 231601.

[32] Van Ginneken B, Armato III S G, de Hoop B, et al. Comparing and combining algorithms for computer-aided detection of pulmonary nodules in computed tomography scans: the ANODE09 study[J]. Medical image analysis, 2010, 14(6): 707-722.

[33] Bunch P C, Hamilton J F, Sanderson G K, et al. A free response approach to the measurement and characterization of radiographic observer performance[C]//Application of optical instrumentation in medicine VI. SPIE, 1977, 127: 124-135.

[34] Niemeijer M, Loog M, Abramoff M D, et al. On combining computer-aided detection systems[J]. IEEE Transactions on Medical Imaging, 2010, 30(2): 215-223.

[35] Ye X, Lin X, Dehmeshki J, et al. Shape-based computer-aided detection of lung nodules in thoracic CT images[J]. IEEE Transactions on Biomedical Engineering, 2009, 56(7): 1810-1820.

[36] Liu Y, Yang J, Zhao D, et al. A method of pulmonary nodule detection utilizing multiple support vector machines[C]//2010 International Conference on Computer Application and System Modeling (ICCASM 2010). IEEE, 2010, 10: V10-118-V10-121.

[37] Shao H, Cao L, Liu Y. A detection approach for solitary pulmonary nodules based on CT images[C]//Proceedings of 2012 2nd International Conference on Computer Science and Network Technology. IEEE, 2012: 1253-1257.

[38] Shaukat F, Raja G, Gooya A, et al. Fully automatic detection of lung nodules in CT images using a hybrid feature set[J]. Medical physics, 2017, 44(7): 3615-3629.

[39] Leader J K, Zheng B, Rogers R M, et al. Automated lung segmentation in X-ray computed tomography: development and evaluation of a heuristic threshold-based scheme1 [J]. Academic radiology, 2003, 10(11): 1224-1236.

[40] Pu J, Roos J, Chin A Y, et al. Adaptive border marching algorithm: automatic lung segmentation on chest CT images[J]. Computerized Medical Imaging and Graphics, 2008, 32(6): 452-462.

[41] Wei Q, Hu Y, Gelfand G, et al. Segmentation of lung lobes in high-resolution isotropic CT images[J]. IEEE Transactions on biomedical engineering, 2009, 56(5): 1383-1393.

[42] Zhao J, Ji G, Qiang Y, et al. A new method of detecting pulmonary nodules with PET/CT based on an improved watershed algorithm[J]. PloS one, 2015, 10(4): e0123694.

[43] Dai S, Lu K, Dong J, et al. A novel approach of lung segmentation on chest CT images using graph cuts[J]. Neurocomputing, 2015, 168: 799-807.

[44] Ju W, Xiang D, Zhang B, et al. Random walk and graph cut for co-segmentation of lung tumor on PET-CT images[J]. IEEE Transactions on Image Processing, 2015, 24(12): 5854-5867.

[45] Mansoor A, Bagci U, Xu Z, et al. A generic approach to pathological lung segmentation[J]. IEEE transactions on medical imaging, 2014, 33(12): 2293-2310.

[46] Rebouças Filho P P, Cortez P C, da Silva Barros A C, et al. Novel and powerful 3D adaptive crisp active contour method applied in the segmentation of CT lung images[J]. Medical image analysis, 2017, 35: 503-516.

[47] W. Zhang, X. Wang, P. Zhang, et al. Global optimal hybrid geometric active contour for automated lung segmentation on CT images[J]. Computers in Biology and Medicine, 2017, 91: 168-180

[48] Silveira M, Nascimento J, Marques J. Automatic segmentation of the lungs using robust level sets[C]//2007 29th Annual International Conference of the IEEE Engineering in Medicine and Biology Society. IEEE, 2007: 4414-4417.

[49] Taşcı E, Uğur A. Shape and texture based novel features for automated juxtapleural nodule detection in lung CTs[J]. Journal of medical systems, 2015, 39: 1-13.

[50] Liu Y., Wang Z., Guo M., et al. Hidden conditional random field for lung nodule detection. In: 2014 IEEE International Conference on Image Processing (ICIP). 2014: 3518–3521

[51] Shi Z, Ma J, Zhao M, et al. Many is better than one: an integration of multiple simple strategies for accurate lung segmentation in CT images[J]. BioMed research international, 2016, 2016(1): 1480423.

[52] Chen X, Udupa J K, Bagci U, et al. Medical image segmentation by combining graph cuts and oriented active appearance models[J]. IEEE transactions on image processing, 2012, 21(4): 2035-2046.

[53] John J, Mini M G. Multilevel thresholding based segmentation and feature extraction for pulmonary nodule detection[J]. Procedia Technology, 2016, 24: 957-963.

[54] Rezaie A A, Habiboghli A. Detection of lung nodules on medical images by the use of fractal segmentation[J]. 2017.

[55] Javaid M, Javid M, Rehman M Z U, et al. A novel approach to CAD system for the detection of lung nodules in CT images[J]. Computer methods and programs in biomedicine, 2016, 135: 125-139.

[56] Wang B, Tian X, Wang Q, et al. Pulmonary nodule detection in CT images based on shape constraint CV model[J]. Medical physics, 2015, 42(3): 1241-1254.

ISSN: 2664-9640

[57] Froz B R, de Carvalho Filho A O, Silva A C, et al. Lung nodule classification using artificial crawlers, directional texture and support vector machine[J]. Expert Systems with Applications, 2017, 69: 176-188.

[58] Khordehchi E A, Ayatollahi A, Daliri M R. Automatic lung nodule detection based on statistical region merging and support vector machines[J]. Image Analysis and Stereology, 2017, 36(2): 65-78.

[59] Liu J, Jiang H, Gao M, et al. An assisted diagnosis system for detection of early pulmonary nodule in computed tomography images[J]. Journal of medical systems, 2017, 41: 1-9.

[60] Farag A A, Ali A, Elshazly S, et al. Feature fusion for lung nodule classification[J]. International journal of computer assisted radiology and surgery, 2017, 12: 1809-1818.

[61] Saien S, Moghaddam H A, Fathian M. A unified methodology based on sparse field level sets and boosting algorithms for false positives reduction in lung nodules detection[J]. International journal of computer assisted radiology and surgery, 2018, 13: 397-409.

[62] Ramachandran S., George J., Skaria S., et al. Using YOLO based deep learning network for real time detection and localization of lung nodules from low dose CT scans. 2018: 53

[63] Fu L., Ma J., Ren Y., et al. Automatic detection of lung nodules: false positive reduction using convolution neural networks and handcrafted features. In: Proc.SPIE. 2017, 10134

[64] Anirudh R, Thiagarajan J J, Bremer T, et al. Lung nodule detection using 3D convolutional neural networks trained on weakly labeled data[C]//Medical Imaging 2016: Computer-Aided Diagnosis. Spie, 2016, 9785: 791-796.

[65] Jenuwine N M., Mahesh S N., Furst J D., et al. Lung nodule detection from CT scans using 3D convolutional neural networks without candidate selection. 2018, 10575: 1057538–1057539

[66] Perez G, Arbelaez P. Automated lung cancer diagnosis using three-dimensional convolutional neural networks[J]. Medical & Biological Engineering & Computing, 2020, 58: 1803-1815.

[67] Huang X., Shan J., Vaidya V. Lung nodule detection in CT using 3D convolutional neural networks. in: 2017 IEEE 14th International Symposium on Biomed Imaging (ISBI 2017). 2017: 379–383

[68] Cao H, Liu H, Song E, et al. A two-stage convolutional neural networks for lung nodule detection[J]. IEEE journal of biomedical and health informatics, 2020, 24(7): 2006-2015.

[69] He K, Zhang X, Ren S, et al. Deep residual learning for image recognition[C]//Proceedings of the IEEE conference on computer vision and pattern recognition. 2016: 770-778.

[70] Tajbakhsh N, Shin J Y, Gurudu S R. Convolutional neural networks for medical image analysis: full training or fine tuning. IEEE Trans Med Imaging, 2016, 35(5): 1299-1312.

[71] Huang G, Liu Z, Van Der Maaten L, et al. Densely connected convolutional networks[C]//Proceedings of the IEEE conference on computer vision and pattern recognition. Honolulu: IEEE. 2017: 4700-4708.

[72] Han Y, Qi H, Wang L, Chen C, Miao J, Xu H, Wang Z, Guo Z, Xu Q, Lin Q, Liu H, Lu J, Liang F, Feng W, Li H, Liu Y. Pulmonary nodules detection assistant platform: An effective computer aided system for early pulmonary nodules detection in physical examination. Comput Methods Programs Biomed. 2022 Apr;217:106680. doi: 10.1016/j.cmpb. 2022. 106680. Epub 2022 Feb 9. PMID: 35176595.

[73] Khosravan N., Bagci U. S4ND: Single-Shot Single-Scale Lung Nodule Detection BT - Medical Image Computing and Computer Assisted Intervention – MICCAI 2018. FRANGI A F, SCHNABEL J A, DAVATZIKOS C, et al. Cham: Springer International Publishing, 2018: 794–802

[74] Zhu W., Liu C., Fan W., et al. DeepLung: Deep 3D Dual Path Nets for Automated Pulmonary Nodule Detection and Classification. in: 2018 IEEE Winter Conference on Applications of Computer Vision (WACV). 2018: 673–681.

[75] Redmon J, Divvala S, Girshick R, et al. You only look once: Unified, real-time object detection[C]//Proceedings of the IEEE conference on computer vision and pattern recognition. 2016: 779-788.

[76] Liu W., Anguelov D., Erhan D., Szegedy C., Reed S., Fu C.Y., Berg A.C. Ssd: Single shot multibox detector; Proceedings of the European Conference on Computer Vision; Amsterdam, The Netherlands. 11–14 October 2016; pp. 21–37.

ISSN: 2664-9640

[77] Bu Z., Zhang X., Lu J., Lao H., Liang C., Xu X., Wei Y., Zeng H. Lung nodule detection based on YOLOv3 deep learning with limited datasets. Mol. Cell. Biomech. 2022;19:17–28. doi: 10.32604/mcb.2022.018318.

[78] Redmon J., Farhadi A. YOLOv3: An Incremental Improvement. arXiv. 20181804.02767

[79] Ren S, He K, Girshick R, et al. Faster R-CNN: towards real-time object detection with region proposal networks[J]. IEEE transactions on pattern analysis and machine intelligence, 2016, 39(6): 1137-1149.

[80] Xie H., Yang D., Sun N., et al. Automated pulmonary nodule detection in CT images using deep convolutional neural networks. Pattern Recognition, 2019, 85: 109–119

[81] Ding J., Li A., Hu Z., Wang L. Accurate pulmonary nodule detection in computed tomography images using deep convolutional neural networks; Proceedings of the International Conference on Medical Image Computing and Computer-Assisted Intervention; Quebec City, QC, Canada. 10–14 September 2017; pp. 559–567.

[82] Tang H., Zhang C., Xie X. Nodulenet: Decoupled false positive reduction for pulmonary nodule detection and segmentation; Proceedings of the International Conference on Medical Image Computing and Computer-Assisted Intervention; Shenzhen, China. 13–17 October 2019; pp. 266–274.

[83] Lin T Y, Dollár P, Girshick R, et al. Feature pyramid networks for object detection[C]//Proceedings of the IEEE conference on computer vision and pattern recognition. 2017: 2117-2125.

[84] Tang S, Yang M, Bai J. Detection of pulmonary nodules based on a multiscale feature 3D U-Net convolutional neural network of transfer learning. PLoS One. 2020 Aug 26;15(8):e0235672. doi: 10.1371/journal.pone.0235672. PMID: 32845877; PMCID: PMC7449493.

[85] Zheng S, Kong S, Huang Z, Pan L, Zeng T, Zheng B, Yang M, Liu Z. A Lower False Positive Pulmonary Nodule Detection Approach for Early Lung Cancer Screening. Diagnostics (Basel). 2022 Nov 1;12(11):2660.

[86] Zhao Y, Wang Z, Liu X, Chen Q, Li C, Zhao H, Wang Z. Pulmonary Nodule Detection Based on Multiscale Feature Fusion. Comput Math Methods Med. 2022 Dec 21;2022:8903037. doi: 10.1155/2022/8903037. PMID: 36590762; PMCID: PMC9797290.

[87] Peng H, Sun H, Guo Y. 3D multi-scale deep convolutional neural networks for pulmonary nodule detection. PLoS One. 2021 Jan 7;16(1):e0244406. doi: 10.1371/journal.pone.0244406. PMID: 33411741; PMCID: PMC7790422.

[88] Li Y., Fan Y. DeepSEED: 3D squeeze-and-excitation encoder-decoder convolutional neural networks for pulmonary nodule detection; Proceedings of the 2020 IEEE 17th International Symposium on Biomedical Imaging (ISBI); Lowa City, IA, USA. 3–7 April 2020; pp. 1866–1869.

[89] Luo X., Song T., Wang G., Chen J., Chen Y., Li K., Metaxas D.N., Zhang S. SCPM-Net: An anchor-free 3D lung nodule detection network using sphere representation and center points matching. Med. Image Anal. 2022;75:102287. doi: 10.1016/j.media.2021.102287.

[90] Huang Y.S., Chou P.R., Chen H.M., Chang Y.C., Chang R.F. One-stage pulmonary nodule detection using 3-D DCNN with feature fusion and attention mechanism in CT image. Comput. Methods Programs Biomed. 2022;220:106786. doi: 10.1016/j.cmpb.2022.106786.

[91] Zhao, Y., Wang, J., Wang, X., Wan, H. (2023). A New Pulmonary Nodule Detection Based on Multiscale Convolutional Neural Network with Channel and Attention Mechanism. In: Sun, J., Wang, Y., Huo, M., Xu, L. (eds) Signal and Information Processing, Networking and Computers. Lecture Notes in Electrical Engineering, vol 917. Springer, Singapore.

[92] Cao, Z., Li, R., Yang, X. et al. Multi-scale detection of pulmonary nodules by integrating attention mechanism. Sci Rep 13, 5517 (2023). doi: 10.1038/s41598-023-32312-1

[93] UrRehman, Z., Qiang, Y., Wang, L. et al. Effective lung nodule detection using deep CNN with dual attention mechanisms. Sci Rep 14, 3934 (2024).

[94] Mkindu, H., Wu, L. & Zhao, Y. Lung nodule detection of CT images based on combining 3D-CNN and squeeze-and-excitation networks. Multimed Tools Appl 82, 25747–25760 (2023).

[95] Hu J., Shen L., Sun G. Squeeze-and-excitation networks; Proceedings of the IEEE Conference on Computer Vision and Pattern Recognition; Salt Lake City, UT, USA. 18–22 June 2018; pp. 7132–7141.

[96] Eun H, Kim D, Jung C, et al. Single-view 2D CNNs with fully automatic non-nodule categorization for false positive reduction in pulmonary nodule detection[J]. Computer methods and programs in biomedicine, 2018, 165: 215-224.

[97] Setio A A A, Ciompi F, Litjens G, et al. Pulmonary nodule detection in CT images: false positive reduction using multi-view convolutional networks[J]. IEEE transactions on medical imaging, 2016, 35(5): 1160-1169.

[98] Dou Q., Chen H., Yu L., Qin J., Heng P.A. Multi-level contextual 3D CNNs for false positive reduction in pulmonary nodule detection. IEEE Trans. Biomed. Eng. 2016;64:1558–1567. doi: 10.1109/TBME.2016.2613502.

[99] Zuo W, Zhou F, He Y. An Embedded Multi-branch 3D Convolution Neural Network for False Positive Reduction in Lung Nodule Detection. J Digit Imaging. 2020 Aug;33(4):846-857. doi: 10.1007/s10278-020-00326-0. PMID: 32095944; PMCID: PMC7522146.

[100] Yuan H, Fan Z, Wu Y, Cheng J. An efficient multi-path 3D convolutional neural network for false-positive reduction of pulmonary nodule detection. Int J Comput Assist Radiol Surg. 2021 Dec;16(12):2269-2277. doi: 10.1007/s11548-021-02478-y. Epub 2021 Aug 27. PMID: 34449037.

[101] Kim B C, Yoon J S, Choi J S, et al. Multi-scale gradual integration CNN for false positive reduction in pulmonary nodule detection[J]. Neural Networks, 2019, 115: 1-10.

[102] Mittapalli P.S., Thanikaiselvan V. Multiscale CNN with compound fusions for false positive reduction in lung nodule detection. Artif. Intell. Med. 2021;113:102017. doi: 10.1016/j.artmed.2021.102017.

[103] Zhao D., Liu Y., Yin H., Wang Z. A novel multi-scale CNNs for false positive reduction in pulmonary nodule detection. Expert Syst. Appl. 2022:117652.

[104] Vipparla V K, Chilukuri P K, Kande G B. Attention Based Multi-Patched 3D-CNNs with Hybrid Fusion Architecture for Reducing False Positives during Lung Nodule Detection[J]. Journal of Computer and Communications, 2021, 9(04): 1.

[105] Gu Z, Li Y, Luo H, et al. Cross attention guided multi-scale feature fusion for false-positive reduction in pulmonary nodule detection[J]. Computers in Biology and Medicine, 2022, 151: 106302.

[106] Sun L., Wang Z., Pu H., Yuan G., Guo L., Pu T., Peng Z. Attention-embedded complementary-stream CNN for false positive reduction in pulmonary nodule detection. Comput. Biol. Med. 2021;133:104357.

[107] Xiao Z., Du N., Geng L., et al. Multi-scale heterogeneous 3D CNN for false-positive reduction in pulmonary nodule detection, based on chest CT images Applied Sciences, 9 (16) (2019), p. 3261

[108] Hao K, Cai A, Feng X, Ma L, Zhu J, Wang M, Zhang Y, Fei B. Lung nodule false positive reduction using a central attention convolutional neural network on imbalanced data. Proc SPIE Int Soc Opt Eng. 2023 Feb;12466:124661X. doi: 10.1117/12.2654216. Epub 2023 Apr 3. PMID: 38487347; PMCID: PMC10940051.

[109] Cao H, Liu H, Song E, et al. Multi-branch ensemble learning architecture based on 3D CNN for false positive reduction in lung nodule detection[J]. IEEE access, 2019, 7: 67380-67391.

[110] Haiying Y, Zhongwei F, Ding D, et al. False-positive reduction of pulmonary nodule detection based on deformable convolutional neural networks[C]//2021 IEEE 9th International Conference on Bioinformatics and Computational Biology (ICBCB). IEEE, 2021: 130-134.